Improved Energy Efficiency via Parallel Elastic Elements for the Straight-legged Vertically-compliant Robot SLIDER

Ke Wang[1], Roni Permana Saputra[1,3], James Paul Foster[2], and Petar Kormushev[1]

[1] Robot Intelligence Lab, Dyson School of Design Engineering, Imperial College London, UK,
[2] Department of Electrical and Electronic Engineering, Imperial College London, UK
[3] Research Center for Electrical Power and Mechatronics, Indonesian Institute of Sciences—LIPI, Bandung, Indonesia
Corresponding author: k.wang17@imperial.ac.uk

Abstract. Most state-of-the-art bipedal robots are designed to be anthropomorphic, and therefore possess articulated legs with knees. Whilst this facilitates smoother, human-like locomotion, there are implementation issues that make walking with straight legs difficult. Many robots have to move with a constant bend in the legs to avoid a singularity occurring at the knee joints. The actuators must constantly work to maintain this stance, which can result in the negation of energy-saving techniques employed. Furthermore, vertical compliance disappears when the leg is straight and the robot undergoes high-energy loss events such as impacts from running and jumping, as the impact force travels through the fully extended joints to the hips. In this paper, we attempt to improve energy efficiency in a simple yet effective way: attaching bungee cords as elastic elements in parallel to the legs of a novel, knee-less biped robot SLIDER, and show that the robot's prismatic hip joints preserve vertical compliance despite the legs being constantly straight. Due to the nonlinear dynamics of the bungee cords and various sources of friction, Bayesian Optimization is utilized to find the optimals configuration of bungee cords that achieves the largest reduction in energy consumption. The optimal solution found saves 15% of the energy consumption compared to the robot configuration without parallel elastic elements. Additional Video: https://youtu.be/ZTaG9_$Dz8A$

Keywords: bipedal robot, parallel elastic, Bayesian optimization

1 INTRODUCTION

A common approach to improve energy efficiency in robots is the inclusion of compliant elements that are capable of storing and subsequently releasing energy at certain points of the robot's gait, performing work that would otherwise have to be taken up by the actuators [1]. In addition to energy efficiency, introducing

compliant elements can also add some degree of robustness, by isolating fragile components of the mechanism from shocks resulting from foot impacts [2] (we explain some exceptions to this later in the introduction). Compliant elements are most commonly used in series, making use of either springs [3], series elastic actuators [4] [5], or oftentimes a combination of both [6] [7]. However, examples of compliant elements in parallel with revolute joints do exist [8] [9], and research into including compliance in the spine of a quadrupedal robot has also been performed [10]. But only simple spring models are used.

Unfortunately, hardware implementation issues (and their workarounds) can often nullify the benefits of energy-saving measures. When attempting to walk with straight (or near straight legs), singularity issues in the robot kinematics may occur [11]. To avoid this situation, robots can often be seen standing and walking in a squatting stance, this is also done to keep the robot's centre of mass at a near constant height for trajectory planning purposes [12]. Furthermore, as an exception to the earlier argument of compliant elements adding robustness to robots, with the leg fully extended, any compliance in the design is severely reduced upon foot touchdown, because impacts travel straight through the links of the leg directly to the hip, bypassing the joint compliance and essentially transferring the impact shock to the torso [13].

This paper is based on the robot SLIDER, shown in Fig. 1, which is a novel straight-legged biped designed by the Robot Intelligence Lab at Imperial College London. In contrast to anthropomorphic biped designs that feature complex, highly articulated legs, SLIDER instead possesses straight, knee-less legs and

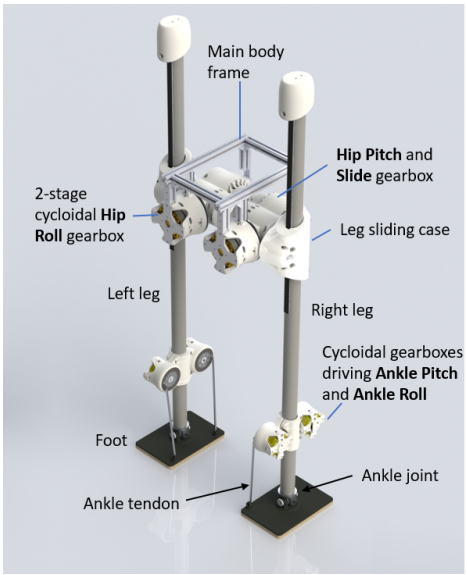

Fig. 1: A model of the SLIDER robot. It has 10 degrees of freedom (DoF) and straight legs made of carbon fiber reinforced polymer. It is designed to be lightweight and suitable for agile locomotion.

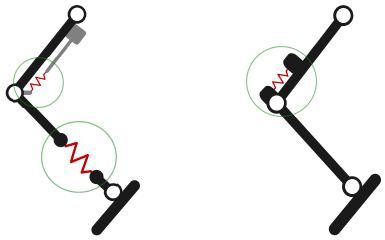

(a) (b)

Fig. 2: Sagittal plane view of common uses of compliant elements in walking robots, circled in green. In (a), compliant elements are either in series with robot links to store energy or dampen impacts, or used as part of series elastic actuators to directly drive joints. In (b), the more rare case of a spring being mounted in parallel with a revolute joint is shown.

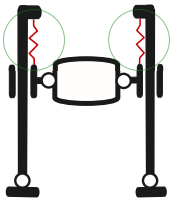

Fig. 3: Coronal plane view showing the novel use of compliant elements in SLIDER, circled in green. As the legs extend above the torso, compliant elements (in this case, bungee cords) can be mounted in parallel with the prismatic joints.

achieves extension by utilizing prismatic joint mechanisms mounted at the hips. Also mounted at the hips are pitch and roll actuators for each leg. The feet are actuated using motors attached higher up the leg to reduce the leg inertia. A more detailed description of the robot can be found in [14] [15].

By leveraging SLIDER's unique design, here we introduce lightweight bungee cords which we anchor in parallel with the prismatic joints that extend the robot's legs, and demonstrate vertical compliance and energy efficiency without the implementation issues seen on robots with articulated legs. To illustrate how our approach differs from the current literature, Fig. 2 shows common uses of compliant elements in legged robots, while Fig. 3 shows our usage of compliant elements on SLIDER. As this paper focuses on compliance with respect to straight legs, for the sake of clarity in Fig. 2 we have omitted any compliant elements acting on the feet (for example in parallel with the ankles), though such elements are important for energy efficiency [16] [17].

Different optimization methods have previously been used in the literature to characterize walking motion that results in energy efficiency. [18] use reinforcement learning with evolving policy parameterization, however the uncertainty is not modelled. [19] use genetic algorithms but this requires a lot of samples.

Bayesian Optimization is a sample-efficient black-box optimization method that can be directly applied onto robot problems [20]. We use Bayesian Optimization for our problem because it works well with dynamics that are hard to model, and it is robust to noisy measurements.

The novelty of this paper lies in:

- the application of parallel elastic elements to straight legs with prismatic joints instead of articulated legs with revolute joints,
- the use of Bayesian Optimization to characterize the optimal vertical motion of SLIDER that results in maximum energy efficiency, taking into account the nonlinear dynamics of the bungee cords and various sources of friction.

2 THE DESIGN OF VERTICAL PRISMATIC JOINT

2.1 Design of The Vertical Prismatic Joint

SLIDER's vertical prismatic joints are designed to be compact, lightweight and backdrivable, this latter property ensures that vertical compliance is always maintained. A single-stage planetary gear provides a 1:4 slide transmission reduction. Inspired by the rack and pinion mechanism, the servo belt mechanism is used, the design detail can be found in [15]. The linear actuation is powered by a tightly meshed pair of 3D printed carbon fiber reinforced plastic double helical gears. The chosen gear type ensures maximum efficiency and low noise production. To increase the contact surface with the pulley, two timing belts are used together, creating a servo belt mechanism. The testing results of the servo belt mechanism are summarized in Table 1.

Table 1: Servo belt test results.

Mass	Max Load	Max Speed	Max Travel Length	Backlash
0.996 Kg	32 Kg	0.45 m/s	0.6 m	negligible

3 CHARACTERISTICS OF THE BUNGEE CORD

3.1 Model of the Bungee Cord

According to [21], the relationship between the applied force on the bungee cord and the length of the cord can be represented using generic stress-strain equations:

$$\sigma = \frac{F}{A} \tag{1}$$

where σ is the stress on the cord, A is the cross-sectional area of the cord when relaxed and F is applied force on the bungee. The strain ε is defined as maximum cord length x divided by the relaxed cord length L:

$$\varepsilon = \frac{x}{L} \tag{2}$$

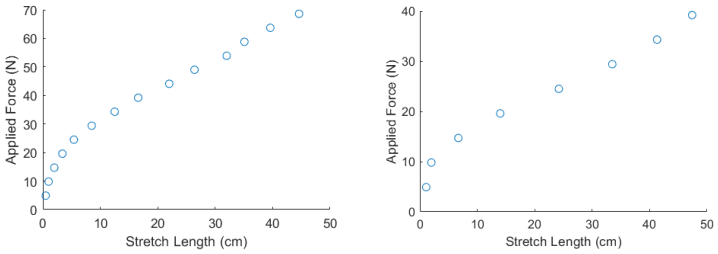

(a) (b)

Fig. 4: Experimental results of bungee cord length change with increasing applied force. In (a), the test results of a bungee cord with a diameter of 10 mm is shown. In (b) the test results of a bungee cord with a diameter of 8 mm was is shown. Both cords have a relaxed length of 40 cm. The results show that the stiffness of the bungee cords is nonlinear with respect to the changing length as force is applied, especially when the stretch length is small.

The modulus of elasticity E is the slope of the stress-strain curve, written as:

$$E = \frac{\sigma}{\varepsilon} \tag{3}$$

The relationship between stiffness k and modulus E is:

$$k = \frac{AE}{L} \tag{4}$$

Compared with the elastic modulus E that is a material property independent of cross-sectional area A and cord length L, according to Eq. 4 the value of stiffness k is dependent on both A and L, making it difficult to calculate the stiffness when the length changes. This is reinforced in Fig. 4, which shows that the bungee cord exhibits nonlinear behaviour.

3.2 Attaching Bungee Cords in Parallel

The design of SLIDER's leg make it easy to attach elastic elements parallel to the leg. The end cap located on the top of each leg and the long bolt of the linear drive hub carriage act as anchor points for attaching the bungee cords, as is shown in Fig. 5. Compared with springs which are widely used as elastic elements on the robots, bungee cords are made of natural rubber and are incredibly light. A unique property of bungee cords is their ability to stretch to roughly six times their relaxed length without breaking, which is an incredibly useful property to have considering the large leg extensions that SLIDER is capable of.

4 FINDING OPTIMAL ENERGY-EFFICIENT CONFIGURATION USING BAYESIAN OPTIMIZATION

4.1 Evaluation of Energy Consumption

The bungee cord can be utilized to improve the energy efficiency of SLIDER's motion, as the cord stores potential energy when it is stretched by downward motion of the pelvis. In order to verify that the robot is saving energy compared to when it does not have bungee cords installed, a way to evaluate energy consumption must be found. One approach is to estimate the mechanical energy from motor torque measurements and angular velocities. However, this approach incorrectly includes the work done by the bungee cord and gravity and can only infer the real electrical energy used for walking indirectly. The approach proposed by us is to directly measure the electrical energy used by the motors of the robot. SLIDER is equipped with open-source ODrive [22] motor controllers, which provide direct measurement of motor current and voltage. The electrical energy can be calculated using the power equation $P = IU$, where I is the electric current and U is the voltage. The consumed energy is calculated by integrating the power over time using

$$E_i = \int_{t_1}^{t_2} I_i(t) U_i(t)\ dt \tag{5}$$

where $[t_1, t_2]$ is the time interval and i is the selected joint for which the energy consumption is calculated. We define one rollout as one walking cycle motion and we performed experiments with multiple rollouts in order to reduce the effect of noise in the measurement. We calculate the average energy consumption of one

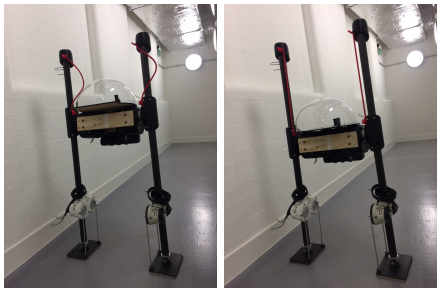

(a) (b)

Fig. 5: SLIDER standing with two different torso heights. When the torso is high in (a), the red bungee cords are relaxed. In (b), the torso is low and the bungee cords are in tension.

cycle, and estimate it using the formula:

$$E(\tau) = \frac{1}{c} \sum_{i \in I} E_i(t_1, t_2) \tag{6}$$

where τ denotes a given rollout of the experiment, I is the set of joints we tested (in our experiment, the vertical slide joint), and c is the number of rollouts included in the experiment.

4.2 Bayesian Optimization for Finding Optimal Energy Efficient Motion

As mentioned in Section 2, the stiffness of the bungee cord is nonlinear with respect to the stretched length. Moreover, mechanical friction from the gearbox and the servo belt is not easy to measure. Both factors make it hard to build a precise dynamic model of SLIDER and optimize the motion analytically. Instead, we use Bayesian Optimization to characterize the stretch length of bungee cords that results in SLIDER being as energy-efficient as possible.

Bayesian Optimization does sequential optimization over a surface response (i.e. surrogate model) instead of optimizing a known objective function directly. The method iteratively creates a data set $D = \{\theta, f(\theta)\}$ in which θ is the parameter and $f(\theta)$ are the corresponding function evaluations. This data set is used to build a surrogate model $\hat{f}(\cdot) : \theta \rightarrow f(\theta)$, that maps θ to the corresponding function evaluations $f(\theta)$. The response surface is subsequently used to replace the optimization of a real objective function which is unknown, with an optimization process which optimizes the surrogate objective function:

$$\theta^* \in_{\theta \in \mathbb{R}} \hat{f}(\theta) \tag{7}$$

We use Gaussian process (GP) [23] as the probabilistic model that allows us to model noisy observations and to explicitly take the uncertainty of the model into account, making the probabilistic model more robust to the effect of model errors. GP also allows us to use priors to encode expert knowledge in a principled way. GP is a distribution defined by the mean and kernel function:

$$f(\mathbf{x}) \sim GP(\mu(\mathbf{x}), k(\mathbf{x}_i, \mathbf{x}_j)), \tag{8}$$

where μ is the mean function and k is the kernel function. The prior mean function $\mu(x)$ is set to be 0 in the experiment. There are a variety of kernel functions to choose from. The most widely used one is the the Squared Exponential (SE) kernel, here we use the Matérn kernel which is a generalization of the SE kernel.

$$k(x_i, x_j) = \sigma^2 \frac{1}{\Gamma(\nu) 2^{\nu-1}} (\gamma \sqrt{2\nu} \rho^{\nu}) K_{\nu}(\gamma \sqrt{2\nu} \rho) \tag{9}$$

where $\rho = d(\frac{x_i}{l}, \frac{x_j}{l})$. This kernel has an additional parameter ν which controls the smoothness of the resulting function, l is the length scale factor which also influences the smoothness of the function.

Given the data set $\mathbb{D} = \{\boldsymbol{X}, \mathbf{y}\}$ with n training inputs where $\mathbf{X} = [\theta_1, ..., \theta_n]$ and corresponding function evaluations $\mathbf{y} = [f_1(\theta), ..., f_n(\theta)]$, the predicted distribution of GP is

$$p(f(\theta) \mid \mathbb{D}, \theta) = \boldsymbol{N}(\mu(\theta), \sigma^2(\theta)), \tag{10}$$

where the mean function $\mu(\theta)$ and the variance σ are:

$$\mu(\theta) = \mathbf{k}_*^T \mathbf{K}^{-1} \mathbf{y}, \sigma^2 = k_{**} - \mathbf{k}_*^T \mathbf{K}^{-1} \mathbf{k}_*, \tag{11}$$

$\mathbf{K}$ is the matrix with $k_{ij} = k(\theta_i, \theta_j)$, $k_{**} = k(\theta, \theta)$ and $\mathbf{k}_* = k(\mathbf{X}, \theta)$.

In order to find next best point to sample, Bayesian Optimization uses an acquisition function $\alpha(\cdot)$. The acquisition function performs a trade-off between exploration and exploitation, which is extremely important for the optimization process when the data set has only a few samples. We use the Upper Confidence Bound (UCB) as the acquisition function because it is reported to be the best performing acquisition function for the task of learning optimal walking gaits [24]. UCB is defined as

$$\alpha(\theta) = \mu(\theta) + \kappa\sigma(\theta) \tag{12}$$

where κ is the factor to trade-off between exploration and exploitation, we will talk about the choice of κ in section 5. The whole Bayesian Optimization algorithm is implemented using an open source package (`https://github.com/fmfn/BayesianOptimization`) and is summarized as Algorithm 1.

Algorithm 1: Bayesian Optimization

Given: A black-box function $f(\theta)$ (defined in Eq. 6) for evaluation, an acquisition function $\alpha(\theta)$ (defined in Eq. 12), maximum iteration.
Output: Current optimal θ^* which minimizes $f(\theta)$.
Initialization: A dataset with pre-collected samples $D = \{\theta_i, f_i\}_{i=1,2,...}$ and find current optimal θ^* and $f(\theta^*)$.
while $i <$ *max_iteration* **do**
  Find next query parameter θ_i by maximizing the acquisition function $\alpha(\theta)$:

$$\theta_i =_\theta \alpha(\theta|D)$$

  Evaluate the objective function $f(\theta)$ at θ_i, if $f(\theta_i) < f(\theta^*)$, then $\theta^* = \theta_i, f(\theta^*) = f(\theta_i)$;
  Add the new data point $\{\theta_i, f(\theta_i)\}$ to the dataset:

$$D \leftarrow D \cup \{\theta_i, f(\theta_i)\}$$

  Update Gaussian Process $GP(\mu(\mathbf{x}), k(\mathbf{x}_i, \mathbf{x}_j))$ and acquisition function $\alpha(\theta)$
  $i = i + 1$
end

5 EXPERIMENTS

We performed experiments directly on SLIDER because in simulation it is very difficult to model the nonlinear dynamics of the bungee cords and the mechanical friction and other losses present in the robot. To measure the improved energy efficiency via the bungee cord, the experiment is conducted using the vertical prismatic joints at the hips[4]. In the experiment setup, we froze all other joints of the robot (hip roll, hip pitch, ankle pitch, ankle roll) by keeping the motor position fixed to 0. For the vertical prismatic joint motion, a bobbing motion was triggered as this motion is similar to the vertical component of walking. To achieve this bobbing motion, the reference trajectory was defined as a sine wave:

$$x(t) = A \sin \omega t + B, \tag{13}$$

where A is the amplitude, ω is the frequency of the sine wave, and B is the vertical offset of the bobbing motion. The value of B equals 0 when the stretch force of the bungee cord equals the sum of the gravitational force and the frictional forces from transmissions. This makes the value of B the same as the default stretched length of the bungee cord.

The bungee cord we used has a diameter of 8 mm at rest and its stiffness can be seen in Fig. 4. We fixed the amplitude A and the frequency ω in order to find the optimal default stretched length of the bungee cord which minimizes the energy consumption via Bayesian optimization. For each trial of Bayesian Optimization we ran 10 rollouts, (recall that one rollout is one period of the sinusoidal motion). The response surface of the Bayesian optimization is the average evaluated energy consumption defined by Eq. 5. The range of B is $[0, 12]$ cm and the relaxed length of the bungee cord is 40 cm. The data is collected sequentially: we first perform one trial and evaluate the energy consumption, then the sample is attached to the data set and fed to the optimizer. The optimizer computes the posterior and gives the value of the B parameter for the next sample using the acquisition function defined by Eq. 12. In our experiments we use $\kappa = 5$ for the collection of the first 5 trials, which means that the optimization process encourages exploration. We changed $\kappa = 1.5$ for later sample collections so that the optimization would prefer exploitation of gathered data.

We performed experiments with two different frequencies representing fast and slow motion. The value of ω in the two experiments is 2.5 rads^{-1} and 5 rads^{-1} respectively, the resultant input and motor trajectories can be seen in Fig. 6. Experimental results show that with bungee cords attached in parallel, the energy efficiency is improved significantly for both fast and slow motion cases, as shown in Fig. 7. In all trials conducted, the energy consumption of the robot with bungee cords attached is smaller than the borderline (energy consumption without attaching bungee cords). In the case of slow motion which has the frequency of 2.5 HZ, the optimal solution computed from only 9 iterations

[4]Due to the COVID-19 pandemic, access to the physical robot has been limited. We thus focus on validating the concept and do not focus on whole-body walking experiments.

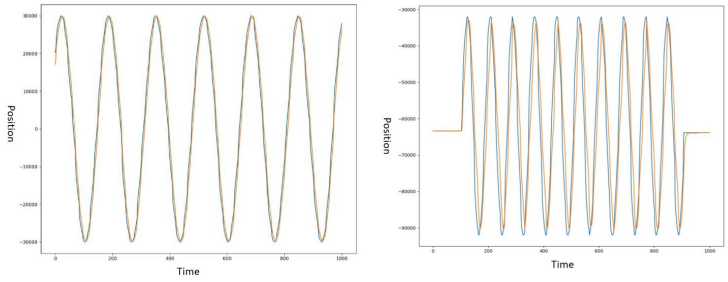

(a) (b)

Fig. 6: Trajectories of the vertical prismatic joint on the left leg in the experiment. The orange line indicates the measured position from the motor while the blue line indicates the desired position. (a) shows the slow motion with a frequency of 2.5 Hz and (b) shows the fast motion with a frequency of 5 Hz.

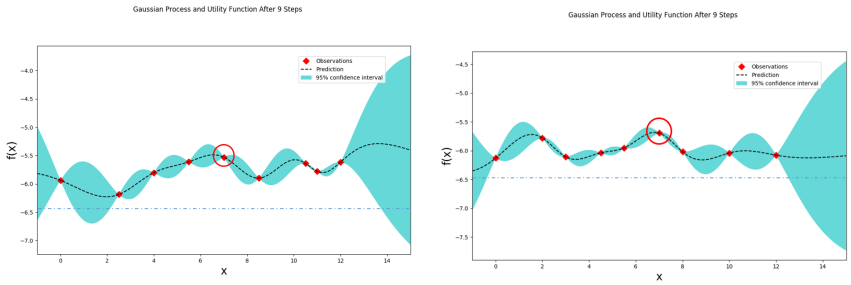

(a) (b)

Fig. 7: Results of the Bayesian Optimization after 9 iterations. (a) shows results of the 2.5 Hz motion and (b) shows results of the 5 Hz motion. The x axis is the vertical offset B and the y axis is the negative value of the evaluation of energy consumption (because the Bayesian Optimization maximizes the objective function). The blue dashed line is the borderline which is the energy consumption without the bungee cord and the red circle indicates the optimal solution.

of Bayesian Optimization, saves 15.5% of SLIDER's energy consumption compared to the borderline. In the case of fast motion which has the frequency of 5 HZ, the optimal solution saves 11.65% of energy consumption compared to the borderline. In both cases, the optimal default stretched length of bungee cords is around 7 cm, indicating that the same bungee cords configuration can be applied onto various speeds. The experimental results are summarized in Table 2.

6 CONCLUSIONS AND FUTURE WORK

We have leveraged the novel design of SLIDER to mount compliant elastic elements (bungee cords) in parallel with prismatic actuation mechanisms, as op-

Table 2: Summary of The Experiment Results.

Frequency (Hz)	2.5	5
Energy Consumption without Bungee Cord (J)	65.43	64.45
Optimal Energy Consumption with Bungee Cord (J)	55.29	56.94
Optimal Default Stretched Length (cm)	6.8	7
Improvement of Energy Consumption (%)	15.5	11.65

posed to current approaches that only consider elastic elements in series, or in parallel with revolute joints. We use Bayesian Optimization to find the optimal configuration of the bungee cords because of the nonlinear dynamics of the elastic elements and various sources of friction. The optimal solution found by only 9 trials is up to 15% more energy-efficient compared to the robot configuration without parallel elastic elements.

In the future, the focus of experiments will be optimizing bungee cords configurations for SLIDER walking and jumping. Another future direction will be co-optimizing the walking motion together with the bungee cords.

References

1. R. Alexander, "Three uses for springs in legged locomotion," *International Journal of Robotics Research*, vol. 9, no. 2, pp. 53–61, 1990.
2. K. Radkhah and O. Von Stryk, "A study of the passive rebound behavior of bipedal robots with stiff and different types of elastic actuation," in *2014 IEEE International Conference on Robotics and Automation (ICRA)*. IEEE, 2014, pp. 5095–5102.
3. K. Sreenath, H.-W. Park, I. Poulakakis, and J. W. Grizzle, "A compliant hybrid zero dynamics controller for stable, efficient and fast bipedal walking on mabel," *The International Journal of Robotics Research*, vol. 30, no. 9, pp. 1170–1193, 2011.
4. G. A. Pratt and M. M. Williamson, "Series elastic actuators," in *Proceedings 1995 IEEE/RSJ International Conference on Intelligent Robots and Systems. Human Robot Interaction and Cooperative Robots*, vol. 1. IEEE, 1995, pp. 399–406.
5. J. Pratt, T. Koolen, T. De Boer, J. Rebula, S. Cotton, J. Carff, M. Johnson, and P. Neuhaus, "Capturability-based analysis and control of legged locomotion, part 2: Application to m2v2, a lower-body humanoid," *The International Journal of Robotics Research*, vol. 31, no. 10, pp. 1117–1133, 2012.
6. D. Hobbelen, T. de Boer, and M. Wisse, "System overview of bipedal robots flame and tulip: Tailor-made for limit cycle walking," in *2008 IEEE/RSJ International Conference on Intelligent Robots and Systems*. IEEE, 2008, pp. 2486–2491.
7. P. Kormushev, B. Ugurlu, D. G. Caldwell, and N. G. Tsagarakis, "Learning to exploit passive compliance for energy-efficient gait generation on a compliant humanoid," *Autonomous Robots*, vol. 43, no. 1, pp. 79–95, 2019.
8. T. Yang, E. R. Westervelt, J. P. Schmiedeler, and R. A. Bockbrader, "Design and control of a planar bipedal robot ernie with parallel knee compliance," *Autonomous robots*, vol. 25, no. 4, p. 317, 2008.
9. A. Mazumdar, S. J. Spencer, C. Hobart, J. Salton, M. Quigley, T. Wu, S. Bertrand, J. Pratt, and S. P. Buerger, "Parallel elastic elements improve energy efficiency on

the steppr bipedal walking robot," *IEEE/ASME Transactions on Mechatronics*, vol. 22, no. 2, pp. 898–908, 2017.
10. G. A. Folkertsma, S. Kim, and S. Stramigioli, "Parallel stiffness in a bounding quadruped with flexible spine," in *2012 IEEE/RSJ International Conference on Intelligent Robots and Systems*. IEEE, 2012, pp. 2210–2215.
11. K. M. Lynch and F. C. Park, *Modern Robotics: Mechanics, Planning, and Control*. Cambridge University Press, 2017.
12. S. Kajita, F. Kanehiro, K. Kaneko, K. Fujiwara, K. Harada, K. Yokoi, and H. Hirukawa, "Biped walking pattern generation by using preview control of zero-moment point," in *2003 IEEE International Conference on Robotics and Automation (Cat. No. 03CH37422)*, vol. 2. IEEE, 2003, pp. 1620–1626.
13. H. Dallali, P. Kormushev, N. Tsagarakis, and D. G. Caldwell, "Can active impedance protect robots from landing impact?" in *Proc. IEEE Intl Conf. on Humanoid Robots (Humanoids 2014)*, Madrid, Spain, 2014.
14. K. Wang, A. Shah, and P. Kormushev, "SLIDER: A bipedal robot with knee-less legs and vertical hip sliding motion," in *Proc. 21st International Conference on Climbing and Walking Robots and Support Technologies for Mobile Machines (CLAWAR 2018)*, Panama, 2018.
15. K. Wang, D. M. Marsh, R. P. Saputra, D. Chappell, Z. Jiang, B. Kon, and P. Kormushev, "Design and control of SLIDER: An ultra-lightweight, knee-less, low-cost bipedal walking robot," in *Proc. IEEE/RSJ Intl Conf. on Intelligent Robots and Systems (IROS 2020)*, Las Vegas, USA, Oct 2020.
16. T. Schauß, M. Scheint, M. Sobotka, W. Seiberl, and M. Buss, "Effects of compliant ankles on bipedal locomotion," in *2009 IEEE International Conference on Robotics and Automation*. IEEE, 2009, pp. 2761–2766.
17. K. Farrell, C. Chevallereau, and E. Westervelt, "Energetic effects of adding springs at the passive ankles of a walking biped robot," in *Proceedings 2007 IEEE International Conference on Robotics and Automation*. IEEE, 2007, pp. 3591–3596.
18. P. Kormushev, B. Ugurlu, S. Calinon, N. G. Tsagarakis, and D. G. Caldwell, "Bipedal walking energy minimization by reinforcement learning with evolving policy parameterization," in *2011 IEEE/RSJ International Conference on Intelligent Robots and Systems*. IEEE, 2011, pp. 318–324.
19. T. Arakawa and T. Fukuda, "Natural motion trajectory generation of biped locomotion robot using genetic algorithm through energy optimization," in *1996 IEEE International Conference on Systems, Man and Cybernetics. Information Intelligence and Systems (Cat. No. 96CH35929)*, vol. 2. IEEE, 1996, pp. 1495–1500.
20. R. Calandra, N. Gopalan, A. Seyfarth, J. Peters, and M. P. Deisenroth, "Bayesian gait optimization for bipedal locomotion," in *International Conference on Learning and Intelligent Optimization*. Springer, 2014, pp. 274–290.
21. J. Kockelman and M. Hubbard, "Bungee jumping cord design using a simple model," *Sports Engineering*, vol. 7, no. 2, pp. 89–96, 2004.
22. Odrive. Odrive robotics. [Online]. Available: https://odriverobotics.com/
23. C. E. Rasmussen, "Gaussian processes in machine learning," in *Summer School on Machine Learning*. Springer, 2003, pp. 63–71.
24. R. Calandra, A. Seyfarth, J. Peters, and M. P. Deisenroth, "An experimental comparison of bayesian optimization for bipedal locomotion," in *2014 IEEE International Conference on Robotics and Automation (ICRA)*. IEEE, 2014, pp. 1951–1958.